

## Forecasting characteristic earthquakes in a minimalist model

M. Vázquez-Prada<sup>1</sup>, Á. González<sup>2</sup>, J. B. Gómez<sup>2</sup>, and A. F. Pacheco<sup>1</sup>

<sup>1</sup>Departamento de Física Teórica and BIFI, Universidad de Zaragoza, Pedro Cerbuna 12, 50009 Zaragoza, Spain

<sup>2</sup>Departamento de Ciencias de la Tierra, Universidad de Zaragoza, Pedro Cerbuna 12, 50009 Zaragoza, Spain

**Abstract.** Using error diagrams, we quantify the forecasting of characteristic-earthquake occurrence in a recently introduced minimalist model. Initially we connect the earthquake alarm at a fixed time after the occurrence of a characteristic event. The evaluation of this strategy leads to a one-dimensional numerical exploration of the loss function. This first strategy is then refined by considering a classification of the seismic cycles of the model according to the presence, or not, of some factors related to the seismicity observed in the cycle. These factors, statistically speaking, enlarge or shorten the length of the cycles. The independent evaluation of the impact of these factors in the forecast process leads to two-dimensional numerical explorations. Finally, and as a third gradual step in the process of refinement, we combine these factors leading to a three-dimensional exploration. The final improvement in the loss function is about 8.5%.

### 1 Introduction

The earthquake process in seismic faults is a very complex natural phenomenon that present geophysics, in spite of its considerable efforts, has not yet been able to put into a sound and satisfactory status. However, in the crucial field of earthquake prediction, recent years have witnessed significant advances. For recent thorough reviews dealing with this issue, see Keilis-Borok (2002); Keilis-Borok and Soloviev (2003), and references therein, in particular chapter four by Kosobokov and Shebalin. See also Lomnitz (1994). The introduction of new concepts coming from modern statistical physics seems to add some light and put some order into the intrinsic complexity of the lithosphere and its dynamics. Thus, for example, references to critical phenomena, dynamical systems, hierarchical systems, fractals, self-organized criticality and self-organized complexity are now found very frequently in geophysical literature (Turcotte, 2000; Sornette, 2000; Gabrielov et al., 1999, 2000). Hopefully, this

conceptual framework will prove its usefulness sooner better than later.

We have recently presented a simple statistical model of the cellular-automaton type which produces an earthquake spectrum similar to the characteristic earthquake behaviour of some seismic faults (Vázquez-Prada et al., 2002). The largest earthquakes on a fault or fault segment (the events that break its complete length) are usually termed characteristic (Schwartz and Coppersmith, 1984; Wesnousky, 1994; Dahmen et al., 1998). For this reason, in the minimalist model the event of maximum size is called the characteristic one. Our model is inspired by the concept of asperity, i.e. by the presence of a particularly strong element in the system which actually controls its relaxation. This model presents some notable properties, some of which will be reviewed in Sect. 2. In Sect. 3, an algebraic procedure for the exact calculation of the probability distribution of the time of return of the characteristic earthquake is presented. The purpose of this paper is to quantify the forecasting of the characteristic earthquake occurrence in this model, using seismicity functions, which are observable, but not stress functions (Ben-Zion et al., 2003), which are not. In Sect. 4, we construct an error diagram (Molchan, 1997; Newman and Turcotte, 2002) based on the time elapsed since the occurrence of the last characteristic event. This permits a first assessment of the degree of predictability. In Sect. 5, we propose a general strategy of classification of the seismic cycles which, adequately exploited in this model, allows a refinement of the forecasts. Finally, in Sect. 6 we present the conclusions.

### 2 Some properties of the model

In the minimalist model (Vázquez-Prada et al., 2002), a one-dimensional vertical array of length  $N$  is considered. The ordered levels of the array are labelled by an integer index  $i$  that runs upwards from 1 to  $N$ . This system performs two basic functions: it is loaded by receiving stress particles in its various levels and unloaded by emitting groups of particles

through the first level  $i = 1$ . These emissions that relax the system are called earthquakes.

These two functions (loading and unloading) proceed using the following four rules:

- i In each time unit, one particle arrives at the system.
- ii All the positions in the array, from  $i = 1$  to  $i = N$ , have the same probability of receiving the new particle. When a position receives a particle we say that it is occupied.
- iii If a new particle comes to a level which is already occupied, this particle has no effect on the system. Thus, a given position  $i$  can only be either non-occupied when no particle has come to it, or occupied when one or more particles have come to it.
- iv The level  $i = 1$  is special. When a particle goes to this first position a relaxation event occurs. Then, if all the successive levels from  $i = 1$  up to  $i = k$  are occupied, and the position  $k + 1$  is empty, the effect of the relaxation (or earthquake) is to unload all the levels from  $i = 1$  up to  $i = k$ . Hence, the size of this relaxation is  $k$ , and the remaining levels  $i > k$  maintain their occupancy intact.

Therefore, the size of the earthquakes in this model range from 1 up to  $N$ , being the event of  $k = N$  the characteristic one. Note that the three first rules of this model are exactly those of the forest-fires model (Drossel and Schwabl, 1992). Our model has no parameter and, at a given time, the state of the system is specified by stating which of the  $(i > 1)N - 1$  ordered levels are occupied. Each one of these possible occupation states corresponds to a stable configuration of the system, and therefore the total number of configurations is  $2^{(N-1)}$ . These mentioned  $2^{(N-1)}$  stable configurations can be considered as the states of a finite, irreducible and aperiodic Markov chain with a unique stationary distribution (Durrett, 1999).

The evolution rules of the model produce an earthquake size-frequency relation,  $p_k$ , that is shown in Fig. 1a, where the results for  $N = 10$ ,  $N = 100$ , and  $N = 1000$  are superimposed. Note that this spectrum has a distribution of the characteristic-earthquake type: it exhibits a power-law relationship for small events, an excess of maximal (characteristic) events, and very few of the intermediate size. Besides, the three superimposed curves of probability are coincident.

The result for the probability of return of the characteristic earthquake,  $P(n)$ , is shown in Fig. 1b for  $N = 20$ . Here  $n$  represents the time elapsed since the last characteristic event. During an initial time interval  $1 \leq n < N$ ,  $P(n)$  is null, then it grows to a maximum and then finally declines asymptotically to 0. (In Sect. 4,  $P(n)$  for  $N = 20$ , will be usually denoted as curve *a*.) In Sect. 3, we explain a general algebraic method for the exact computation of  $P(n)$ .

The configurations of the model are classified into groups according to the number of levels,  $j$ , that are occupied

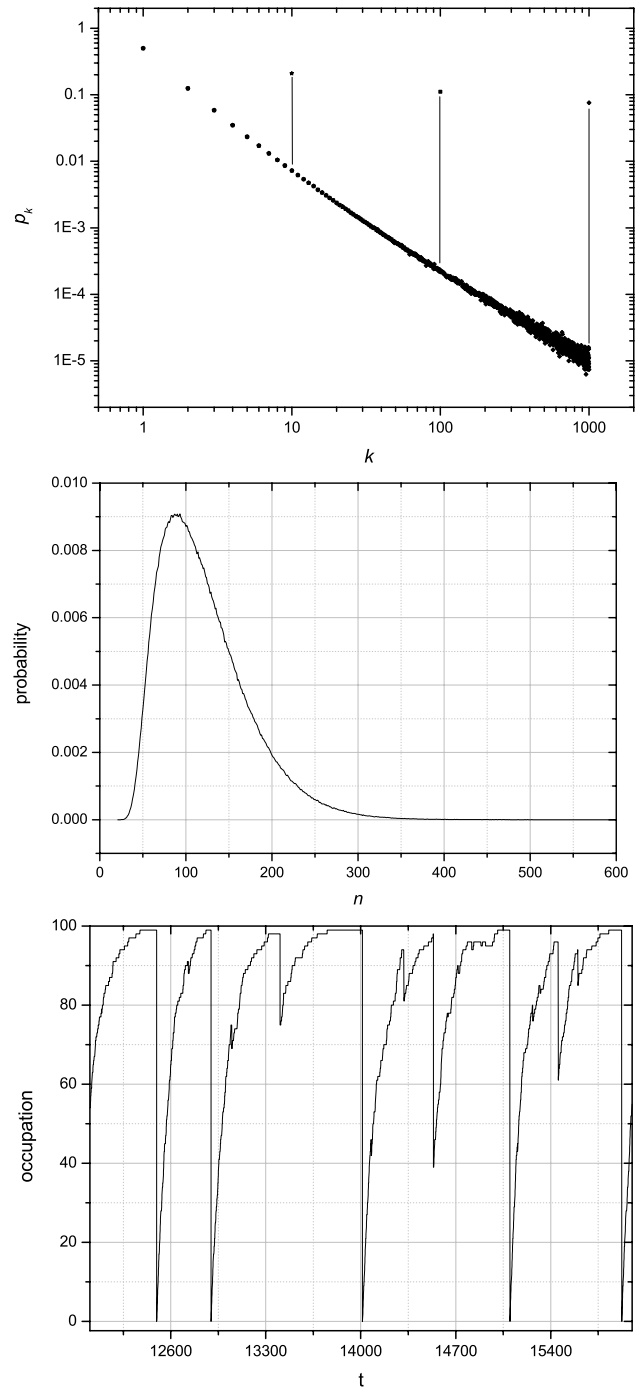


**Fig. 1.** (a) Probability of occurrence of earthquakes of size  $k$ . Note that the simulations corresponding to  $N$  equal to 10, 100, and 1000 are superimposed. (b) For  $N = 20$ , the probability of return of the characteristic earthquake as a function of the time elapsed since the last event,  $n$ . (c) Time evolution of the state of occupation in a system of size  $N = 100$ . Note that after each characteristic event that completely depletes the system, there follows the corresponding recovery up to a high level of occupancy, and then the system typically presents a plateau previous to the next characteristic earthquake.

( $0 \leq j \leq N - 1$ ). Using the Markov-chain theory or producing simulations (Vázquez-Prada et al., 2002), one easily observes that in this model the system resides often in the configurations of maximum occupancy, i.e. in  $j = N - 2$  and  $j = N - 1$ .

This last property can be observed in Fig. 1c, where we have represented, for  $N = 100$ , the time evolution of the level of occupancy,  $j$ , in an interval long enough to observe the occurrence of several characteristic earthquakes. The typical pattern after a total depletion is a gradual recovery of  $j$  up to a new high level of occupancy. Once there, the system typically presents a plateau before the next characteristic earthquake. Especially during the ascending recoveries, the level of occupancy  $j$  suffers small falls corresponding to the occurrence of rather small earthquakes, that in this model are abundant. Of course, one also observes that occasionally  $j$  falls in a significant way corresponding to the occurrence of a  $N > k \geq N/2$  intermediate earthquake.

Due to the fact that this model is not critical, it is reasonable to consider it as an example of self-organized complexity (Gabrielov et al., 1999).

### 3 Algebraic approach to $P(n)$

The function  $P(n)$ , for a minimalist system of size  $N$ , is obtained from the Markov matrix of the system,  $\mathbf{M}$ , following the following three steps: (i) The element of the last row and first column of  $\mathbf{M}$  is changed by a 0. After this pruning, the matrix will be called  $\mathbf{M}'$ . (ii) The new matrix  $\mathbf{M}'$  is multiplied by itself  $n - 1$  times to obtain  $\mathbf{M}'^{(n-1)}$  and the element of the first row, last column of this matrix is identified. (iii)  $P(n)$  is the product of this selected matrix element times  $1/N$ .

The whys of this recipe are explained in Vázquez-Prada et al. (2002), where  $P(n)$  for  $N = 2$  is explicitly obtained by mere inspection. The result is

$$P(n) = \frac{n-1}{2^n}, \quad N = 2. \quad (1)$$

The explicit form of  $P(n)$  for larger values of  $N$ , can be achieved by exploiting the Jordan decomposition of  $\mathbf{M}'$ ,

$$\mathbf{M}' = \mathbf{Q} \mathbf{J} \mathbf{Q}^{-1}, \quad (2)$$

and hence,

$$\mathbf{M}'^{n-1} = \mathbf{Q} \mathbf{J}^{n-1} \mathbf{Q}^{-1}. \quad (3)$$

The matrix  $\mathbf{J}$  is formed by “Jordan blocks” in the diagonal positions, i.e. by square matrices whose elements are zero except for those on the principal diagonal, which are all equal, and those on the first superdiagonal, which are equal to unity. Thus, the task of obtaining an arbitrary power of  $\mathbf{J}$  is simple because, as said, each Jordan block is the sum of two commuting matrices: one is a constant times the unity matrix, and the other is nilpotent. Therefore, in the computation of any arbitrary power of  $\mathbf{J}$ , each block is independent and the corresponding Newton binomial formula can be applied.

As an example, we now present the calculation of the case  $N = 3$ . In this case,

$$3\mathbf{M}' = \begin{pmatrix} 1 & 1 & 1 & 0 \\ 0 & 2 & 0 & 1 \\ 1 & 0 & 1 & 1 \\ 0 & 0 & 0 & 2 \end{pmatrix}, \quad (4)$$

which is decomposed as

$$\begin{pmatrix} 1 & 1 & 1 & 0 \\ 0 & 2 & 0 & 1 \\ 1 & 0 & 1 & 1 \\ 0 & 0 & 0 & 2 \end{pmatrix} = \begin{pmatrix} -1 & 1 & 1 & 2 \\ 0 & 0 & 2 & -1 \\ 1 & 1 & 0 & 0 \\ 0 & 0 & 0 & 2 \end{pmatrix} \begin{pmatrix} 0 & 0 & 0 & 0 \\ 0 & 2 & 1 & 0 \\ 0 & 0 & 2 & 1 \\ 0 & 0 & 0 & 2 \end{pmatrix} \begin{pmatrix} -1/2 & 1/4 & 1/2 & -3/8 \\ 1/2 & -1/4 & 1/2 & 3/8 \\ 0 & 1/2 & 0 & 1/4 \\ 0 & 0 & 0 & 1/2 \end{pmatrix}. \quad (5)$$

Therefore,

$$\mathbf{J}^{n-1} = \begin{pmatrix} 0 & 0 & 0 & 0 \\ 0 & 2^{n-1} & (n-1)2^{n-2} & 1/2(n-1)(n-2)2^{n-3} \\ 0 & 0 & 2^{n-1} & (n-1)2^{n-2} \\ 0 & 0 & 0 & 2^{n-1} \end{pmatrix} \left(\frac{1}{3}\right)^{n-1}, \quad (6)$$

and from Eq. (3)

$$\mathbf{M}_{1,4}^{n-1} = \frac{2^n}{32} (n-2)(n+5) \left(\frac{1}{3}\right)^{n-1}. \quad (7)$$

Thus, finally,

$$P(n) = \left(\frac{2}{3}\right)^n \frac{(n-2)(n+5)}{32}, \quad N = 3. \quad (8)$$

One could optimistically guess that  $P(n)$ , for an arbitrary  $N$ , can be deduced from the systematics observed in the previous low- $N$  cases. This is disproved by the following formula, which is the result of  $P(n)$  for  $N = 4$ .

$$P(n) = \left(\frac{1}{4}\right)^n \left[ -\frac{13}{16} + \frac{7n}{4} - \frac{n^2}{2} + \frac{n^3}{32} + 3^n \left[ -\frac{3}{16} + \frac{7n}{324} + \frac{n^2}{108} + \frac{n^3}{2599} \right] \right], \quad N = 4. \quad (9)$$

Although it is not apparent, this formula, as it should, vanishes for  $n = 3$ . As in Eqs. (1) and (8),  $P(n)$  in Eq. (9) is adequately normalized:

$$\sum_{n=N}^{\infty} P(n) = 1. \quad (10)$$

### 4 Error diagram for the forecasting of the characteristic earthquake

In the following paragraphs, we will stick to a model of size  $N = 20$  to make the pertinent comparisons. This size is big enough for our purposes here, and small enough to obtain good statistics in the simulations.

For  $n = 20$  the mean value of  $P(n)$  is

$$\langle n \rangle = \sum_{i=20}^{\infty} P(i)i = 121.05, \quad (11)$$

the standard deviation is

$$\sigma = \left[ \sum_{i=20}^{\infty} P(i)(i - \langle n \rangle)^2 \right]^{1/2} = 55.21, \quad (12)$$

and the skew of the distribution is

$$\gamma = \frac{1}{\sigma^3} \sum_{i=20}^{\infty} P(i) \cdot (i - \langle n \rangle)^3 = -0.10. \quad (13)$$

Now we enter into the matter of forecasting. As in any optimization strategy, we will try to achieve simultaneously the most in a property called A and the least in a property called B, these two purposes being contradictory in themselves. Here A is the (successful) forecast of the characteristic earthquakes produced in the system. Our desire is to forecast as many as possible, or ideally, all of them. B is the total amount of time that the earthquake alarm is switched on during the forecasting process. As is obvious, our desire would be that this time were a minimum. The maximization of A is equivalent to the minimization of an  $A'$  that represents the fraction of unsuccessful forecasts.

Thus, in practice, our goal in this paper is to obtain simultaneously a minimum value for the two following functions,  $f_e$  and  $f_a$ . The first represents the fraction of unsuccessful forecasts, or fraction of failures; the second represents the fraction of alarm time. These two functions, in this first one-dimensional strategy of forecasting, are dependent only on the value of  $n$ , that is, the time elapsed since the last main event, and to which the alarm is connected. Using the function  $P(n)$  previously defined, they read as follows:

$$f_e(n) = \sum_{n'=1}^n P(n'), \quad (14)$$

$$f_a(n) = \frac{\sum_{n'=n}^{\infty} P(n') (n' - n)}{\sum_{n'=0}^{\infty} P(n') n'}. \quad (15)$$

These two functions are plotted in Fig. 2a. By eliminating  $n$  between  $f_e(n)$  and  $f_a(n)$ , we obtain Fig. 2b, which is the standard form of representing the so-called error diagram. The diagonal straight line would represent the result of a random forecasting strategy. The curved line is the result of this model.

Error diagrams were introduced in earthquake forecasting by Molchan who contributed with rigorous mathematical analysis to the optimization of the earthquake prediction strategies (Molchan, 1997). In his papers Molchan used  $\tau$  and  $n$  to represent the alarm fraction and the error fraction respectively; and put  $\tau$  in the horizontal axis.

To fix ideas, it is convenient to define a so-called loss function,  $L$ , which expresses the trade-off between costs and benefits in the forecasting (Keilis-Borok, 2002). Among all the possible loss functions, we will choose the simple linear function

$$L = f_a + f_e. \quad (16)$$

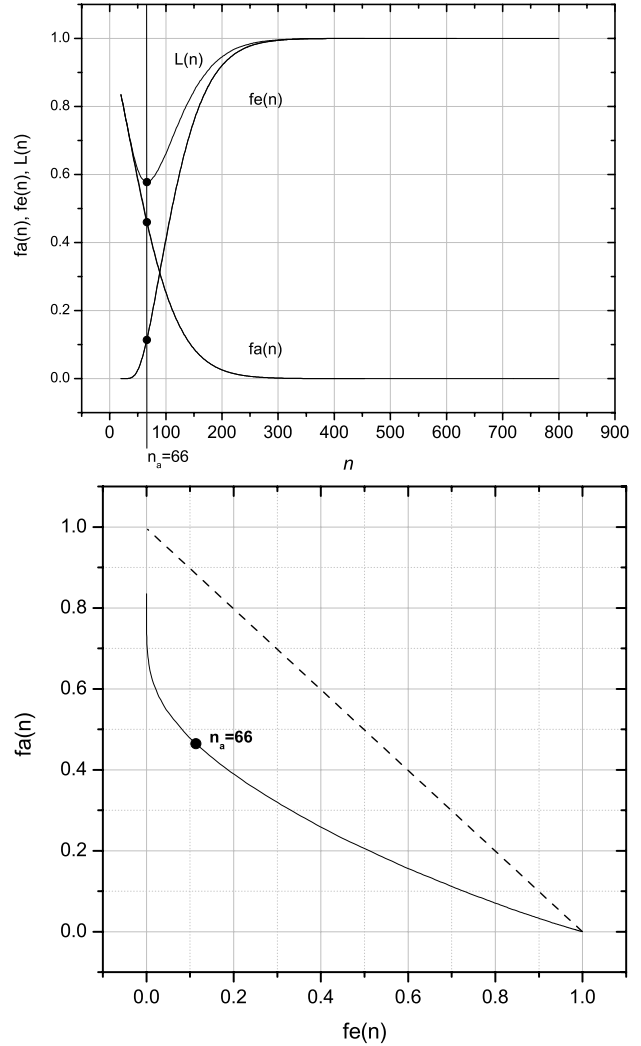


**Fig. 2.** For  $N = 20$ , (a) Fraction of failures to predict,  $f_e$ , fraction of alarm time,  $f_a$ , and loss function  $L = f_a + f_e$  as a function of  $n$ . (b) Error diagram for characteristic event forecasts based on  $n$ . The diagonal line would correspond to a random strategy.

$L(n)$  is also drawn in Fig. 2a. The position  $n_a = 66$  provides the minimum value of  $L(n)$ .  $L(n_a) = 0.578$ . Note that  $n_a$  does not coincide either with the  $n$  that maximizes  $P(n)$ , or with  $\langle n \rangle$ .

## 5 Improving the forecasts

In Sect. 4 we adopted the strategy of connecting the alarm at a fixed time,  $n$ , after the occurrence of a characteristic event. The evaluation of this strategy leads to the conclusion that for  $n = n_a = 66$ , the loss function has a minimum value  $L(n_a) = 0.578$ . The question now is: Can we think up other strategies that render better results? To answer this question, we now return to our previous comments on Fig. 1.

If we define a medium-size earthquake as an event with a size between  $N/2$  and  $N - 1$ , i.e.  $N > k \geq N/2$ , by observing the graphs in Fig. 1, one is led to the conclusion that in this model the occurrence of a medium-size earthquake is not frequent but when it actually takes place, the time of return of the characteristic quake in that cycle is increased.

This qualitative perception can be substantiated by numerically obtaining the probability of having cycles where no medium-size earthquake occurs, i.e.  $k < N/2$ . This information is completed by the distribution of cycles where the condition  $N > k \geq N/2$  does occur. These two distributions are shown in Fig. 3a as lines *b* and *c* respectively. Here, line *a* represents the total distribution of the times of return of the characteristic earthquake in this model (the same as plotted in Fig. 1b). Note that, as it should, the distribution *a* covers both distributions *b* and *c*. The mean time  $\langle n \rangle$  for the three distributions is  $\langle n \rangle_a = 121.05$ ,  $\langle n \rangle_b = 107.57$  and  $\langle n \rangle_c = 166.84$ . The fraction of cycles under *b* is 0.77 and the fraction under *c* is 0.23. A splitting of this type, in which the *a* distribution separates into *b* and *c*, will be denoted henceforth as  $a = b \oplus c$ .

To check if  $a = b \oplus c$  is potentially useful for our purposes, we will now analyze independently these two sets of cycles, *b* and *c*, with the method used in Sect. 4 for curve *a*. The result is the following: the best working *n* for dealing with the cycles under distribution *b* is  $n_b = 60$ . And with respect to the cycles belonging to the distribution under *c*, the best *n* is  $n_c = 124$ .

Therefore, we will now study again the whole set of cycles, i.e. those under *a*, by means of a retarding strategy, which is based on the splitting  $a = b \oplus c$ . We will adopt the following steps: in any cycle, we will wait until an *n*, named  $n_{ret1}$  (which is near to  $n_b$ ), before taking any decision. If no medium earthquake has occurred so far, then the alarm is connected at  $n_{ret1}$ . If, on the contrary, a medium quake has occurred before  $n_{ret1}$ , then we move the alarm to  $n_{ret2}$  (which is close to  $n_c$ ). This notation  $n_{ret1}$  and  $n_{ret2}$  comes from the retarding strategy that we are exploring now. This two-dimensional strategy is implemented by varying  $n_{ret1}$  and  $n_{ret2}$  looking for the best value of *L*. This is illustrated in Fig. 4a. The best option is  $n_{ret1} = 61$  and  $n_{ret2} = 101$ , with  $L(n_{ret1}, n_{ret2}) = 0.549$ .

Now we look for a similar property that can classify the cycles from another point of view. This new property consists in identifying the cycles where the sum of the sizes of all the earthquakes before the characteristic one is less than  $N/2$ . This condition will be represented by  $SUM < N/2$ . The reason for this choice is that if  $SUM < N/2$ , the system, statistically speaking, tends to reach more rapidly the configurations of maximum occupancy,  $j = N - 2$  and  $j = N - 1$ , and the time of return of the characteristic quake in that cycle tends to be smaller (see Fig. 1c). In Fig. 3b, line *a* represents, as in Fig. 3a, the distribution of return intervals of the characteristic earthquake for all the cycles of the model. And lines *f* and *g* represent, respectively, the separation of line *a* according to the fulfilment, or not, of the  $SUM < N/2$  condition,  $a = f \oplus g$ . The mean value of the *f* and *g* dis-

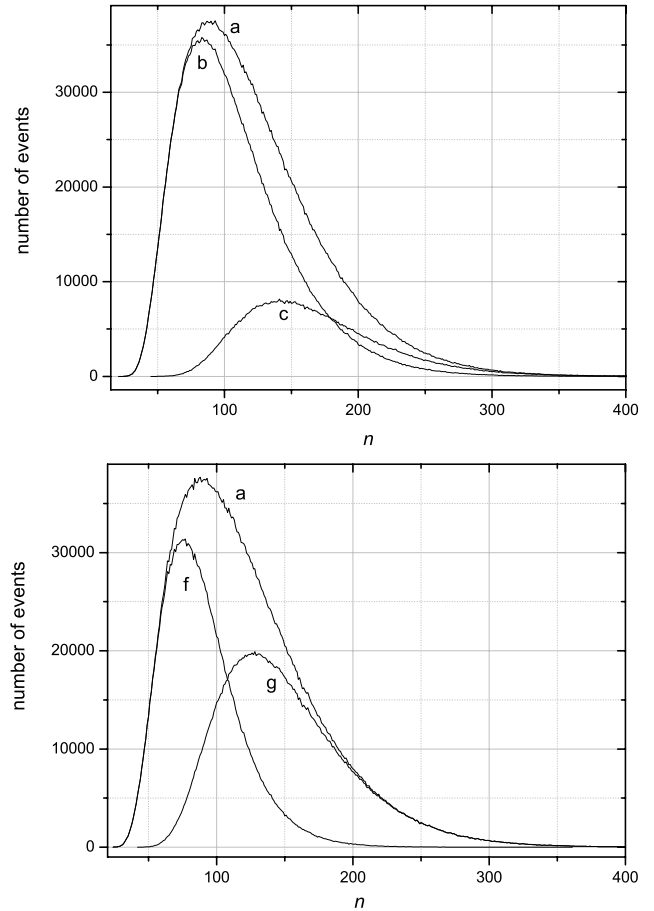


**Fig. 3.** (a) For  $N = 20$ . Line *a* is the distribution of return times of the characteristic earthquake as a function of the time elapsed since the last event, *n*. Line *b* corresponds to the distribution of cycles where no medium-size earthquake occurs. Line *c* corresponds to cycles with medium-size earthquakes. Curves *b* and *c* constitute the splitting of curve *a* according to whether this retarding effect is fulfilled or not. (b) Lines *f* and *g*, represent the separation of the *a* distribution according to whether the advancing effect is fulfilled or not.

tributions is  $\langle n \rangle_f = 88.78$  and  $\langle n \rangle_g = 151.69$  respectively. The fraction of events under the *f* and *g* lines is 0.37 and 0.63 respectively.

This second splitting of the whole set of cycles in the model,  $a = f \oplus g$ , can be used as an advancing strategy in parallel to what we did with the retarding strategy. Thus the independent analysis of curve *f* leads to  $n_f = 60$ , and the similar analysis of curve *g* leads to  $n_g = 90$ .

We will now study again the whole set of cycles (under *a*) by means of the advancing strategy, which is based on the splitting  $a = f \oplus g$ . Therefore, we proceed as follows: In any cycle, we wait until  $n_{adv1}$  (which is close to  $n_f$ ) before taking any decision. If the condition  $SUM < N/2$  has been fulfilled, then the alarm is connected at  $n = n_{adv1}$ . If, on the contrary, this condition has not been fulfilled, then we move the alarm to  $n_{adv2}$  (which is close to  $n_g$ ). This

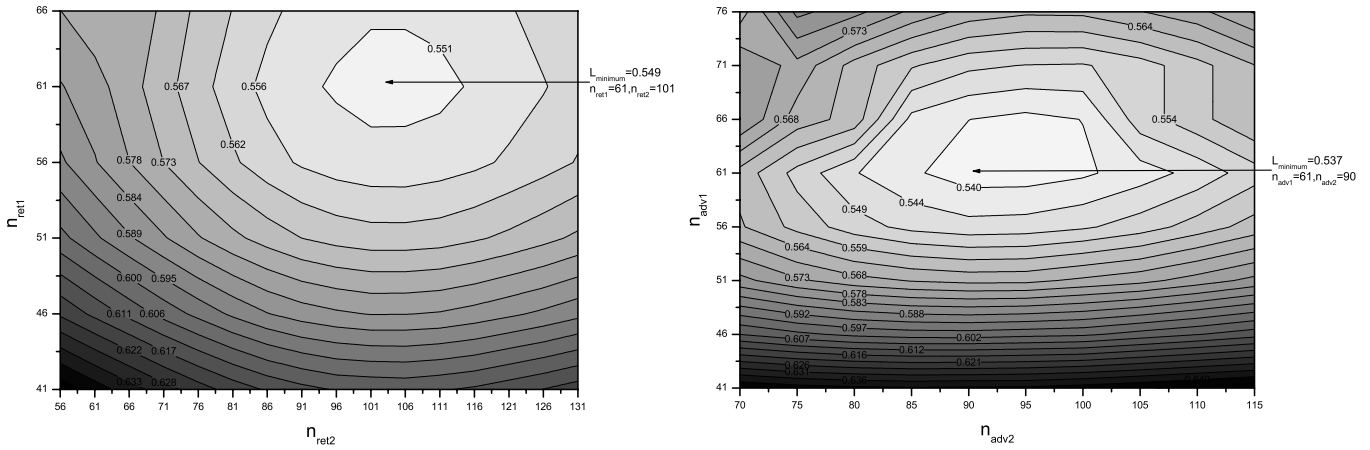


**Fig. 4.** (a) For  $N = 20$ . Results of the two-dimensional strategy based on the splitting of curve  $a$  according to whether the retarding effect is fulfilled or not. Values of  $L$  varying  $n_{ret1}$  and  $n_{ret2}$ . Minimum value of  $L = 0.549$  for  $n_{ret1} = 61$  and  $n_{ret2} = 101$ . (b) Results of the two-dimensional strategy based on the splitting of curve  $a$  according to whether the advancing effect is fulfilled or not. Values of  $L$  varying  $n_{adv1}$  and  $n_{adv2}$ . Minimum value of  $L = 0.537$  for  $n_{adv1} = 61$  and  $n_{adv2} = 90$ .

two-dimensional strategy is implemented by varying  $n_{adv1}$  and  $n_{adv2}$  looking for the lowest  $L$ . This is illustrated in Fig. 4b. The search for the best option leads to  $n_{adv1} = 61$  and  $n_{adv2} = 90$ , with  $L(n_{adv1}, n_{adv2}) = 0.537$ . This value of  $L$  is slightly better than that obtained using the retarding strategy.

Inspired by these results, we will now analyze the possibilities of a mixed strategy which contains conceptual elements of the two partial strategies discussed so far. Here we will explore a 3-dimensional grid of points  $(n_1, n_2, n_3)$  looking for the minimization of  $L$ . The first coordinate,  $n_1$ , will be explored in the neighbourhood of  $n_{adv1}$ , the second coordinate  $n_2$  in the neighbourhood of  $n_{adv2}$ , and finally  $n_3$  near  $n_{ret2}$ . The two successive key decisions to be taken are:

- i In any cycle, we wait until  $n = n_1$ . If  $SUM < N/2$  IS fulfilled, we connect the alarm at  $n_1$  and leave it there. If at  $n = n_1$ ,  $SUM < N/2$  is NOT fulfilled, we move the alarm to  $n_2$ . And,
- ii (We are now at  $n_2$ ). If no medium-size event has occurred between  $n_1$  and  $n_2$ , we leave the alarm connected at  $n_2$ . If, on the contrary, one or more medium-size events have occurred in this interval, then we move the alarm to  $n_3$ .

The search for the triplet  $(n_1, n_2, n_3)$  that makes  $L$  minimum is illustrated in Fig. 5. The result corresponds to  $(n_1 = 61, n_2 = 84, n_3 = 104)$ , and there,  $L = 0.528$ . This is the best result obtained in this work.

Thus, the improvement obtained in  $L$ , when passing from  $L(n_a)$  to  $L(n_1, n_2, n_3)$  is around  $\simeq 8.5\%$ .

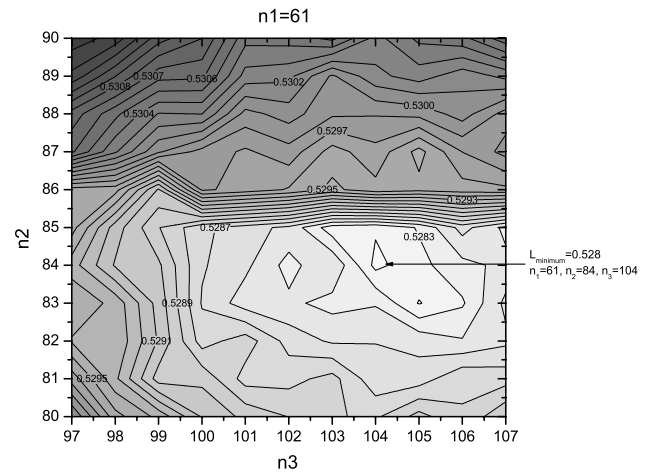


**Fig. 5.** For  $N = 20$ . Illustration of the three-dimensional strategy. For  $n_1 = 61$ ,  $L$ -constant level-curves are plotted. The minimum value of  $L$  is 0.528 for  $n_1 = 61$ ,  $n_2 = 84$ ,  $n_3 = 104$ .

## 6 Conclusions

In this paper, we have analyzed the behaviour of the minimalist model in relation to a quantitative assesment of the forecasting of its successive characteristic earthquakes. We have chosen a simple loss function,  $L = f_a + f_e$ . Our first try, based on a one-dimensional search in  $n$ , produces a minimum result of  $L$  around 0.578. This was illustrated in Fig. 2a. With the aim of improving the forecasts, we then explored two modes of a common strategy that divides the probability distribution of the time of return of the characteristic earthquake into two distinct distributions. The first mode consists in using the occurrence of intermediate-magnitude earthquakes as

a sign that the characteristic earthquake would likely return at a time later than usual in that cycle. This is based on the fact that medium-size events significantly deplete the load in the system and its recovery induces a retardation. This effect takes place in any system of the sand-pile type. The exploitation of this idea leads to a two-dimensional search that finally renders an  $L$  value around 0.549 (Fig. 4a). The second idea consists in using the fact that a significant absence of small earthquakes during a sizeable lapse of time in the cycle is a sign of imminence of the next characteristic event, or at least of a shortening of its period of return. This strategy is similar to the old wisdom in seismology that links a steady absence of earthquakes in a fault with the increase in the risk of occurrence of a big event. The exploration of this idea proceeds similarly to what we did with the retarding strategy: this also leads to a two-dimensional search. It renders a minimum  $L$  around 0.537. (Fig. 4b).

Finally, a mixed strategy that tries to incorporate the information acquired is implemented by means of a three-dimensional search, and provides a value of  $L = 0.528$ . The identification of the three optimum parameters is illustrated in Fig. 5.

It is important to remark that the information we have used in our forecasts is based only in the observed systematics of earthquake occurrence in the model, i.e. only seismicity functions have been used. Thus, for example, in Sect. 5 we have not used the state of occupancy of the system  $j$ , which would have given much more accurate predictions. In real life, the use of this information would be equivalent to knowing, in real time, the value of the stress level and the failure threshold at any point in a fault.

*Acknowledgements.* We are grateful to the two Referees of the first version of this paper for their thorough and helpful reviews. This work was supported by the project BFM2002-01798 of the Spanish Ministry of Science. Miguel Vázquez-Prada and Álvaro González are respectively supported by the PhD research grants B037/2001 (funded by the Autonomous Government of Aragón and the European Social Fund) and AP2002-1347 (funded by the Spanish Ministry of Education).

## References

- Ben-Zion, Y., Eneva, M., and Liu, Y.: Large earthquake cycles and intermittent criticality on heterogeneous faults due to evolving stress and seismicity, *J. Geophys. Res.*, 108 (B6), 2307, doi: 10.1029/2002JB002121, 2003.
- Dahmen, K., Ertas, D., and Ben-Zion, Y.: Gutenberg-Richter and characteristic behavior in simple mean-field models of heterogeneous faults, *Phys. Rev.*, E58, 1444–1501, 1998.
- Drossel, B. and Schwabl, F.: Self-organized critical forest-fire model, *Phys. Rev. Lett.*, 69, 1629–1632, 1992.
- Durrett, R.: *Essentials of Stochastic Processes*, Chapter 1, Springer, 1999.
- Gabrielov, A., Newman, W. I., and Turcotte, D. L.: Exactly soluble hierarchical clustering model: inverse cascades, self-similarity and scaling, *Phys. Rev.*, E60, 5293–5300, 1999.
- Gabrielov, A., Zaliapin, I., Newman, W., and Keilis-Borok, V. I.: Colliding cascades model for earthquake prediction, *Geophys. J. Int.*, 143, 427–437, 2000.
- Keilis-Borok, V.: Earthquake prediction: state-of-the-art and emerging possibilities, *Annu. Rev. Earth Planet. Sci.*, 30, 1–33, 2002.
- Keilis-Borok, V. I. and Soloviev, A. A. (Eds): *Nonlinear Dynamics of the Lithosphere and Earthquake Prediction*, Springer, 2003.
- Lomnitz, C.: *Fundamentals of Earthquake Prediction*, J. Wiley & Sons, 1994.
- Molchan, G. M.: Earthquake prediction as a decision-making problem, *Pure. Appl. Geophys.*, 149, 233–247, 1997.
- Newman W. I. and Turcotte, D. L.: A simple model for the earthquake cycle combining self-organized complexity with critical point behavior, *Nonlin. Proces. Geophys.*, 9, 453–461, 2002.
- Schwartz, D. P. and Coppersmith, K. J.: Fault behaviour and characteristic earthquakes: Examples from the Wasatch and San Andreas Fault Zones, *J. Geophys. Res.*, 89, 5681–5698, 1984.
- Sornette, D.: *Critical Phenomena in Natural Sciences*, Springer Verlag, Berlin, Germany, 2000.
- Turcotte, D. L.: *Fractals and Chaos in Geology and Geophysics*, 2nd Edit., Cambridge Univ. Press, 2000.
- Vázquez-Prada, M., González, Á., Gómez, J. B., and Pacheco, A. F.: A Minimalist model of characteristic earthquakes, *Nonlin. Proces. Geophys.*, 9, 513–519, 2002.
- Wesnousky, S. G.: The Gutenberg-Richter or characteristic-earthquake distribution, which is it?, *Bull. Seism. Soc. Am.*, 84, 1940–1959, 1994.